JOURNAL OF GEOPHYSICAL RESEARCH, VOL. 103, NO. A5, PAGES 9567-9574, MAY 1, 1998

Correlative study of solar activity and cosmic ray intensity

I. G. Usoskin[1]

Sezione di Milano, INFN, Milano, Italy

H. Kananen, K. Mursula and P. Tanskanen

Department of Physical Sciences, University of Oulu, Oulu, Finland

G. A. Kovaltsov

A. F. Ioffe Physical-Technical Institute, St.Petersburg, Russia

Abstract. We perform a correlative study of solar activity (sunspot numbers) and cosmic ray intensity (neutron monitor count rates) for the last four solar cycles. Analysis of the running cross correlation between the two series shows that the behavior of cosmic ray modulation is similar, in general, for particles with different energy. However, a strong rigidity dependence as well as an unusual behavior of the cross correlation function is found for the descending phase of cycle 20. We study the evolution of cosmic ray and solar activity cycles in a three-dimensional phase space by means of the delayed component method. While all solar activity cycles and most cosmic ray cycles are planar, cosmic ray cycle 20 is significantly three-dimensional. A concept of the momentary phase of a cycle is introduced, and the phase evolution of cosmic ray and solar activity cycles is studied. We also discuss the heliospheric conditions responsible for the unusual behavior of cosmic ray modulation in the descending phase of cycle 20.

1. Introduction

It has been known for a long time that the intensity as well as the energy spectrum of galactic cosmic rays (CR) is modulated by solar activity (SA). Although the problem of modulation has been studied both theoretically and experimentally for more than 30 years, it is still a subject of intense research. In the present paper we perform, using new techniques, a detailed correlative study of the recorded time series of cosmic ray intensity and solar activity for the last four solar cycles. We use monthly means of neutron monitor (NM) count rates as an index of CR (Figure 1a). The world network of ground-based neutron monitors provides very stable and reliable records of intensities of CR particles of different energy (rigidity) for more than a 40-year period. In this paper, when speaking of CR particles, we mean particles detected by ground-based neutron monitors (within the energy range from several hundred MeV up to several tens of GeV). We use monthly means of sunspot (Wolf) numbers as an index of SA (Figure 1b).

While the overall negative correlation between CR and SA is well known, details of the temporal behavior of this correlation are of particular interest. In section 2 we will study the running cross correlation between CR and SA as a function of time. We will analyze fine details of the cross correlation for different CR energies and find an unusual correlation during the descending phase of cycle 20.

[1]On leave from A. F. Ioffe Physical-Technical Institute, St. Petersburg, Russia.

Paper number 97JA03782.
0148-0227/98/97JA-03782$09.00

The fact that both CR and SA series have an overall 11-year periodicity let us study the topological features of the time evolution of these series in a three-dimensional (3-D) phase space by means of the series [*Kurths and Ruzmaikin*, 1990; *Ostryakov and Usoskin*, 1990; *Mundt et al.*, 1991; *Kremliovsky*, 1994; *Usoskin et al.*, 1997], but in section 3 of the present paper we perform the first joint analysis of the evolution of CR and SA series in a 3-D phase space. We find the outstandingly 3-D nature of CR cycle 20.

Because of the large size of the heliosphere and diffusive/drift propagation of cosmic ray particles, there is a time lag between the SA and CR series [e.g., *Dorman and Dorman*, 1967] which, as well as the amplitude of the modulation, varies from cycle to cycle [e.g., *Nagashima and Morishita*, 1979]. It is also well known that the lag is larger for odd and smaller for even cycles. However, the usual methods do not reveal the fine temporal structure of the lag. In section 4 of the present paper we study the momentary time lag between the two series, using the momentary phase approach introduced earlier [*Usoskin et al.*, 1997]. In section 5 we will discuss the results, in particular, the unusual behavior of CR during the descending phase of cycle 20.

2. Cross Correlation Between CR and SA As a Function of Time

It is well known that the time series of CR intensity follows, with some time delay, the inverse time profile of solar activity. This is due to the modulation of galactic cosmic rays by the Sun. To study this correlation in more detail, we have calculated the running cross-correlation coefficient between the monthly NM count rates and monthly sunspot numbers (Wolf series). We use a time window of width T centered at time t: $[t-T/2, t+T/2]$. The cross-correlation coefficient $C(t)$ is calculated for data within this window. Then the window is shifted in time by a small time

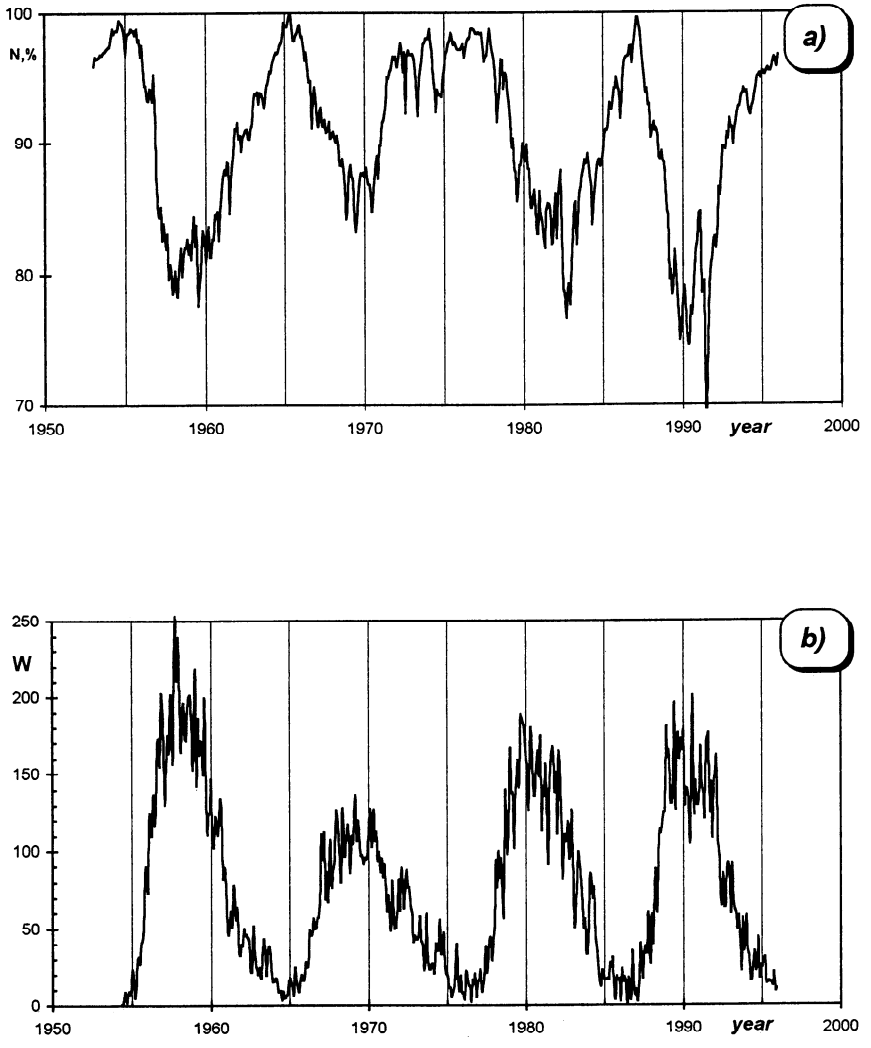

Figure 1. The original data series (monthly means) used in the present paper: (a) cosmic ray intensity recorded by Climax neutron monitor (NM) and (b) sunspot (Wolf) numbers.

step $\Delta t<T$, and the new value of the cross-correlation coefficient is calculated. In this study we use the time window of T=50 months. This value was chosen to match two contradictory requirements: (1) uncertainties of the calculated $C(t)$ are smaller for larger T and (2) T should be small in order to reveal the fine temporal structure of the cross-correlation function. No time shift between the two series is used when calculating the cross-correlation coefficients.

The running cross-correlation function $C(t)$ between the Climax NM and sunspot numbers is shown in Figure 2a. The dotted line denotes the 95% confidence interval for the coefficient $C(t)$. One can see a quasiperiodic behavior of the correlation function with a period of about 5.5 years, half of 11-year cycle. While the connection between SA and CR is strong ($|C|\approx$0.8-0.9) during ascending and descending phases of SA cycles, the correlation becomes weak ($|C|<$0.2-0.4) during extrema (minima and maxima) of SA cycles. This 5.5-year quasiperiodicity in the cross-correlation function is only an artifact due to the delay of the CR series with respect to SA and the fast change of the time series near the extrema. (There is no significant 5.5-year periodicity in SA [see, e.g., *Mursula et al.*, 1997].)

One can see in Figure 2a that the correlation coefficient became significantly positive (C=0.4±0.2) in 1981. This can be explained as follows (see Figure 3): The minimum CR intensity was expected in 1981, about a year after the corresponding SA maximum. However, there was a sudden deep decrease in neutron monitor count rate in 1982 due to a series of strong Forbush decreases in summer-fall of 1982. This led to an unexpectedly late minimum of the smoothed CR series (second half of 1982) with respect to the corresponding SA maximum (end of 1979). Therefore, during the period of 1979-1982, both the smoothed CR intensity and SA were decreasing (Figure 3), leading to a positive correlation.

Another period of an unusual behavior of the cross-correlation function is observed in the descending phase of cycle 20 (1972-1976). During this period the correlation was weak and exceptionally long. Also, the cross-correlation function had an additional local maximum during this period in contrast to a smooth development during all other cycles. This special period of the descending phase of cycle 20 will be discussed in more detail in section 5.

We have also studied the dependence of CR/SA correlation on the energy (rigidity) of cosmic ray particles. We have

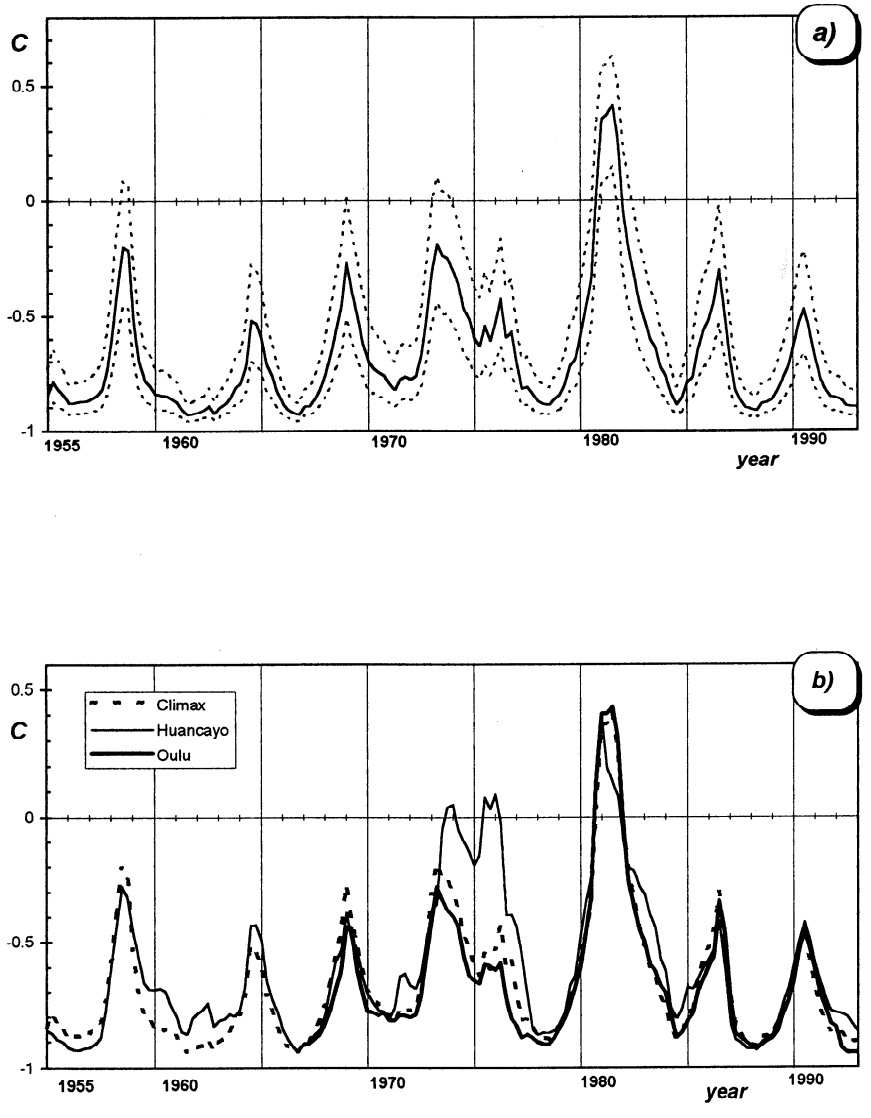

Figure 2. Running cross-correlation function between solar activity (SA) and cosmic ray (CR) time series for (a) Climax monitor count rates, in which solid line shows the most probable value and dashed lines show the 95% confidence interval and (b) most probable values for neutron monitors with different cutoff rigidities: Huancayo (13 GV), Climax (3 GV), and Oulu (< 1 GV).

calculated the cross-correlation function for three neutron monitors with different geomagnetic cutoff rigidities (R). Figure 2b shows the correlation functions for Climax ($R\approx3$ GV), the high-latitude Oulu ($R<1$ GV), and the equatorial Huancayo ($R\approx13$ GV) neutron monitors. It is seen that all the three curves coincide fairly well with each other within the 95% confidence interval for the entire interval except for the particular period of 1972-1977. This good overall coincidence means that the general behavior of CR modulation is similar for particles with different energies (within the energy range of neutron monitor sensitivity) even if the depth of the modulation changes with particle energy.

Let us now analyze the temporal behavior of $C(t)$ at the three stations during the special period of 1972-1977 (Figure 2b). Oulu and Climax neutron monitors depict a very similar pattern with a minimum anticorrelation in 1973 ($|C|\approx0.2$-0.3), followed by a slow, nonmonotonous recovery of anticorrelation level to $|C|\approx0.9$ in 1978. However, the temporal behavior of $C(t)$ for Huancayo monitor is quite different from the two, higher-latitude stations during this period. In 1972-1973 the correlation between the Huancayo monitor count rate and SA decreased roughly to zero and remained at zero level until 1976. During 1976-1977 the correlation at Huancayo NM recovered very fast up to $|C|\approx0.9$. We also note that during the whole period of 1972-1977 the level of anticorrelation at Oulu NM was slightly but systematically higher than that at Climax NM. Accordingly, we suggest that in 1972-1977 the CR modulation by solar activity became weaker with increasing particle energy and disappeared for particle rigidities above about 10 GV.

3. 3-D Portraits of SA and CR Intensity Cycles

Both solar activity and cosmic ray intensity are strongly quasiperiodical (11 years). Therefore it is of great interest to study the behavior of this cyclicity in a 3-D phase space. For this purpose we use the delayed component method which allows one to reconstruct from a single time series a multidimensional trajectory which is similar, in a topological sense, to the actual

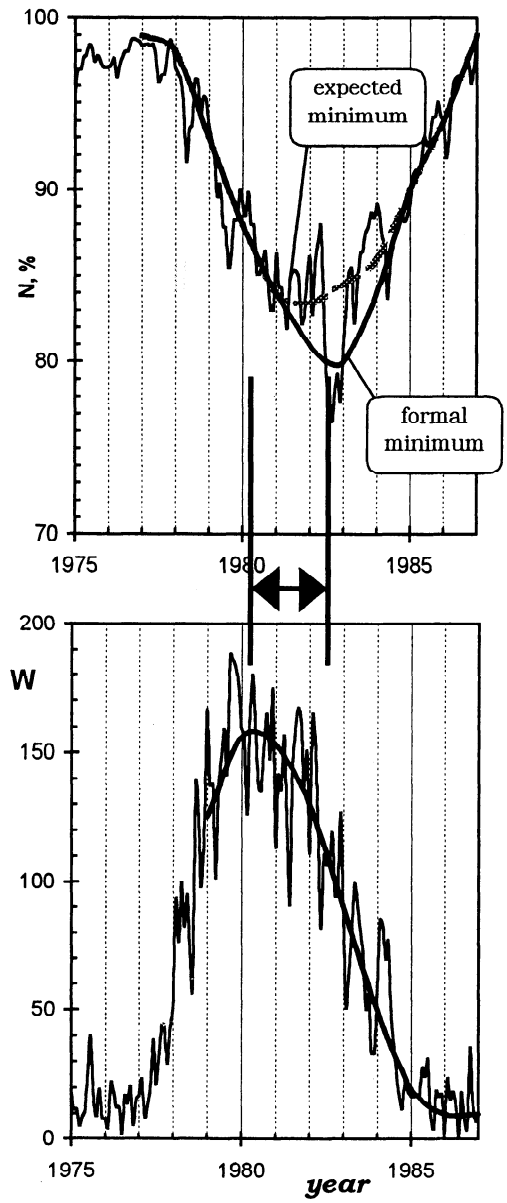

Figure 3. Illustration of positive correlation between CR and SA in 1981. The arrow within the vertical solid lines denotes the period when the slopes of the two series had same sign. (top) Climax monitor count rates (solid line corresponds to the smoothed curve of actual observations; dashed line gives the expected curve). (bottom) The sunspot numbers for the same period.

trajectory of the system in an n-dimensional phase space. The method of time-delayed components is based on the Packard-Takens procedure [*Packard et al.*, 1980]. From a time series of observations (one-dimensional realization of a dynamical system) $\{x_i\}$ a series of n-dimensional vectors $\{X_i \equiv (x_i, x_{i+\tau}, \ldots, x_{i+(n-1)\tau})\}$ can be constructed. According to the theorem by *Takens* [1981] the evolution of $\{X_i\}$ is similar, from the topological point of view, to the actual evolution of the system in an n-dimensional phase space. Thus the method allows one to study the evolution of an n-dimensional dynamical system using a one-dimensional time series. The point X_i corresponds to the momentary state of the system in the n-dimensional phase space. Note that this method in a two-dimensional (2-D) case is similar to that of an oscilloscope which uses an original signal in the X input and the delayed signal in the Y input. In the case of a harmonic signal with period T the oscilloscope depicts a cycle on the screen if the delay time $\tau = \frac{1}{4}T$.

The 3-D trajectories of solar activity and cosmic ray intensity (Climax monitor) are shown in Figures 4 and 5, respectively. Both series were smoothed for the analysis. The time delay was chosen to be $\tau = 30$ months which is close to the first zero of the autocorrelation function and roughly one quarter of the main period (11 years). Figures 4 and 5 depict the last four solar cycles. Note that although data until 1996 were included, the trajectories end as early as in 1991 because the effective length of the 3-D curve is 2τ shorter than the original series by construction. One can see that both curves are rather smooth and have a clear cyclic behavior. The trajectory of solar activity evolution (Figure 4) is very regular and in a good agreement with 3 D portraits of SA constructed earlier [*Kurths and Ruzmaikin*, 1990; *Kremliovsky*, 1994]. The trajectory of cosmic ray intensity evolution (Figure 5) is also smooth and cyclic but more complicated.

Let us now compare the temporal evolution of the two series during cycle 19 (1954-1964). The three-dimensional SA cycle (Figure 4) was large, round, and planar (essentially two-dimensional). The 3-D evolution during this SA cycle was rather uniform as depicted by the fact that the stippled circles denoting the beginning of the year are uniformly distributed along the curve. The corresponding three-dimensional CR cycle had an average amplitude and was egg-shaped and planar. The evolution around the top of the cycle (1958-1959) was somewhat slower than during the rest of the cycle. We have summarized the general features (amplitude, shape, and planarity) of each cycle in Table 1.

Cycle 20 is of particular interest since it has been noted to be unusual in CR modulation [e.g., *Webber and Lockwood*, 1988;

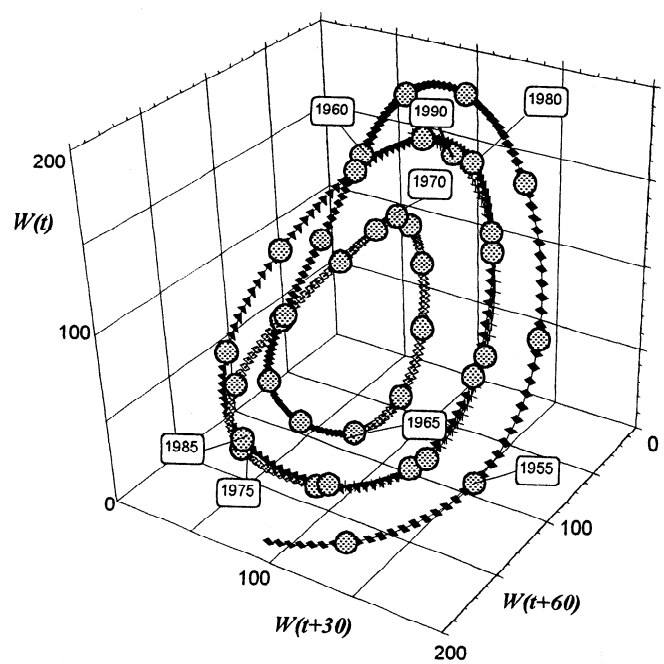

Figure 4. Evolution of SA cycles in a 3-D phase space using the delayed component technique. Large stippled circles denote the January month of each year.

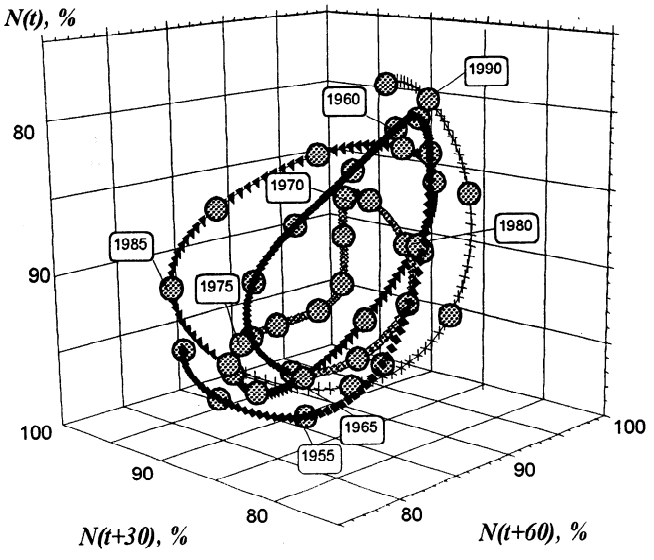

Figure 5. As in Figure 4 but for cosmic rays.

Usoskin et al., 1997]. The 3-D evolution of this SA cycle was of small amplitude and planar. The evolution slowed down slightly at the top of the cycle (1969-1970). However, the 3-D behavior of the corresponding CR cycle is much more complicated. While a more detailed analysis of this cycle will be given in section 5, we would like to mention that this CR cycle is essentially three-dimensional, in contrast to other cycles that are planar. Therefore a 2-D treatment of this cycle is not sufficient.

Solar activity cycles 21 and 22 are known to be very similar to each other in their sunspot number evolution. We note that these two cycles also coincide with each other, at least up to the time available presently, even in 3-D space. Moreover, the rate of evolution along the trajectory was the same for both cycles. This is illustrated by the fact that the stippled circles corresponding to the beginning of the ith year of cycle 21 coincide with the points corresponding to the $(i+10)$th year of cycle 22 (i.e., 1975 and 1985, 1976 and 1986, etc.). This gives us an opportunity to study the possible difference in CR modulation between an odd and a subsequent similar even cycle. Although SA cycles 21 and 22 coincide with each other, the corresponding CR cycles differ from each other, depicting the different modulation for odd and even cycles.

4. Phase Evolution of CR and SA Cycles

As was discussed in section 3, the 3-D cycles 19-22 of both SA and CR are planar except for CR cycle 20 (see also Table 1). This implies that most cycles can be projected onto a 2-D plane without a change in their topological features. *Usoskin et al.* [1997] discussed the 2-D evolution of CR and SA. The special period in the descending phase of cycle 20 was seen in the 2-D evolution of CR series [*Usoskin et al.*, 1997, Figure 2] as a separate small loop. They also introduced the concept of a momentary phase of a cycle using its evolution in the two-dimensional plane and preliminarily estimated the evolution of this phase for CR and SA cycles.

Let us now present how to calculate the momentary phase φ (see Figure 6). SA cycle 21, which was very regular and smooth, was chosen to illustrate the method. The momentary phase φ gives the rotation angle of the point along the curve in two dimensions. First, the center of the cycle is determined. We define the center to be the mass center of the cycle, irrespective of the distribution of points on the cycle, that is, as if it was made of a thin wire. Note that this center is not equal, in general, to the mass center of cycle points which obviously depends on the distribution of the points along the cycle. The center is the reference point when calculating the momentary phase φ of the cycle, and φ=0 denotes the beginning of the cycle. Thus, for every moment t, one can calculate the corresponding phase $\varphi(t)$ (see Figure 6). Note that the phase corresponding to the end of a cycle may differ slightly from 2π, as is shown in Figure 6. This is because a SA cycle is typically slightly overlapping with its neighboring cycles as seen in, for instance, the Maunder butterfly diagram. This implies that a cycle can be slightly underrotated or overrotated. This procedure is repeated for each cycle.

The momentary phases for SA and CR cycles 19-22 calculated as described above are presented in Figure 7. Note that because the effective length of the 2-D curve is 2τ shorter than the original series (see section 3), there is an uncertainty when calculating the center of cycle 22. Therefore the results for cycle 22 should be considered only as preliminary. It is seen from Figure 7 that there is a general delay of the CR phase with respect to SA except for a exceptional period in cycle 20 when the phase of CR was ahead of the SA phase.

The momentary time lag between the moments of equal phase of SA and CR cycles can be defined as sketched in Figure 7: (1) for a certain time t_S, the phase φ of the SA cycle is determined; (2) the time t_C of the same phase is found for CR cycle; and (3) the difference $t_C - t_S$ is the momentary time lag between SA and CR cycles. Note that small gaps in the time lag may appear near the end of a cycle because for some moment t_S close to the end of a SA cycle the phase φ for SA may exceed the maximum phase for the corresponding CR cycle. In such a case the time lag cannot be calculated at the end of the SA cycle.

The temporal behavior of the time lag between SA and CR series is shown in Figure 8 for two neutron monitors with

Table 1. Properties of 3-D Evolution Cycles of Solar Activity and Cosmic Ray Intensity

	Solar Activity			Cosmic Ray Intensity		
Cycle	Amplitude	Shape	Planarity	Amplitude	Shape	Planarity
19	large	round	planar	average	egg-like	planar
20	small	round	planar	small	round	3-D
21	average	round	planar	average	egg-like	planar
22	coincides with cycle 21	coincides with cycle 21	coincides with cycle 21	large	round	planar

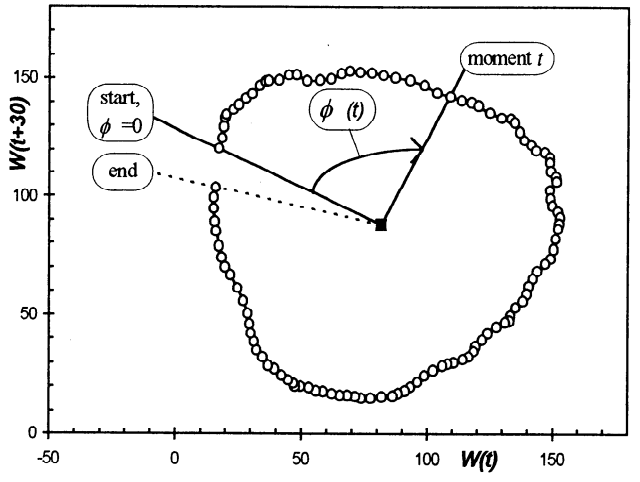

Figure 6. Definition to calculate the momentary phase of the cycle.

different geomagnetic cutoff rigidities: Climax (≈3 GV) and Huancayo (≈13 GV). (As noted above, the results for cycle 22 are preliminary.) Note that the concept of momentary time lag between CR and SA series presented here differs from time lags reported earlier, for example, by *Nagashima and Morishita* [1979], *Lopate and Simpson* [1991], and *Nymmik and Suslov* [1995]. Their methods were to minimize the correlation coefficient between the two series. Such an approach only yields a time lag which is averaged over one full cycle. The present method gives the lag at every moment of time. If the momentary time lag (Figure 8) is integrated over a full SA cycle, a good agreement is found with the average lag obtained by other authors. (Note also that Figure 8 slightly differs from our previous preliminary results [*Usoskin et al.*, 1997] because we now use a more precise formal approach. The fact that the earlier and present results are very close to each other implies that the phase evolution is only slightly dependent on technical details.)

5. Discussion and Conclusions

The 3-D evolution plots (Figures 4 and 5) represent well the long-term behavior of SA and CR. One can see in Table 1 that all SA cycles studied are round and approximately planar, but the amplitude varies from small (cycle 20) to large (cycle 19). Moreover, the planes of the SA cycles are oriented very similarly to each other. The CR cycles studied are, except for cycle 20, also planar, but the plane orientations are quite different. The amplitude of a CR cycle reflects that of the corresponding SA cycle. However, the shapes of CR cycles are different: round for even and egg-like for odd cycles. This is related to the more sinusoidal character of the even CR cycles (see Figure 1a). The even CR cycles have relatively short (≤2 years) and sharp minima, while the odd cycles have longer (3-4 years) minima, making them less sinusoidal.

The exact coincidence of SA cycles 21 and 22 (at least to the point presently available) lets one to study the difference in CR modulation between odd and even cycles under similar SA conditions. As seen in Figure 5 and in Table 1, CR cycles 21 and 22 differ both in shape and amplitude. This further verifies that the sign of the global magnetic field polarity is important for CR modulation.

As already noted in section 4, the CR evolution shows a qualitatively different behavior during the descending phase of cycle 20 (1970-1976). During this special period a singularity occurred in the CR evolution. Note that an unusual "minicycle" in CR during 1973-1974 has been reported earlier [e.g., *Webber and Lockwood*, 1988]. In contrast to all other CR and SA cycles (see Table 1), CR cycle 20 was significantly three-dimensional. Its evolution curve deviates from planarity in 1969 and restores it in 1975. Since this cycle is not planar, its topological features are changed when projecting onto a 2-D plane (which was necessary, e.g., when studying the phase of evolution). This topological change leads to the appearance of a small self-crossing loop in the 2-D curve of CR cycle 20 [*Usoskin et al.*, 1997] and to the negative phase lag (Figure 8) during this particular period. Formally, this means that the phase of SA cycle was late with respect to the CR cycle. This peculiarity is clearly seen in the phase evolution (Figure 7) when, after 1969, the CR momentary phase was growing up very fast until 1972 and then remained at that level for about 3 years. In 1974 the SA phase reached the CR phase, and after 1975 their evolution was quite normal. Zero and negative slope of the CR phase in 1973-1974 corresponds to the self-crossing loop in the 2-D curve. This peculiarity in phase evolution is due to the very fast CR recovery after the maximum of SA cycle 20 (1969-1970) while the SA level was slowly decreasing. One can see from the raw CR data

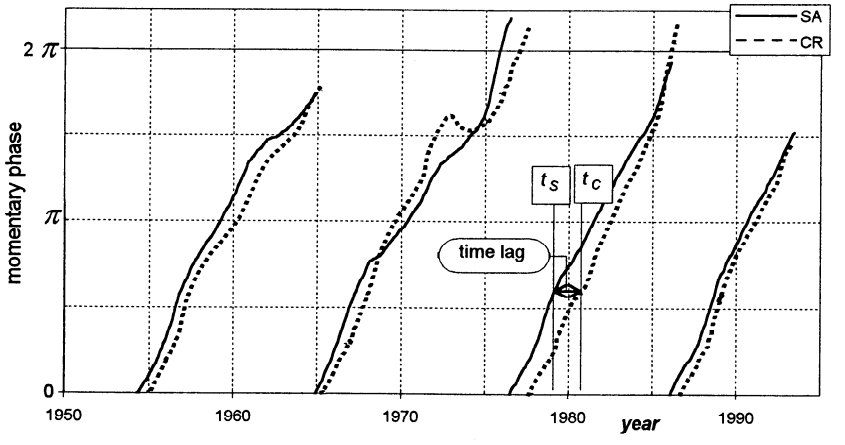

Figure 7. Momentary phases of SA (solid lines) and CR (dashed lines) cycles. A scheme to calculate the time lag between the moments of equal phase is also shown.

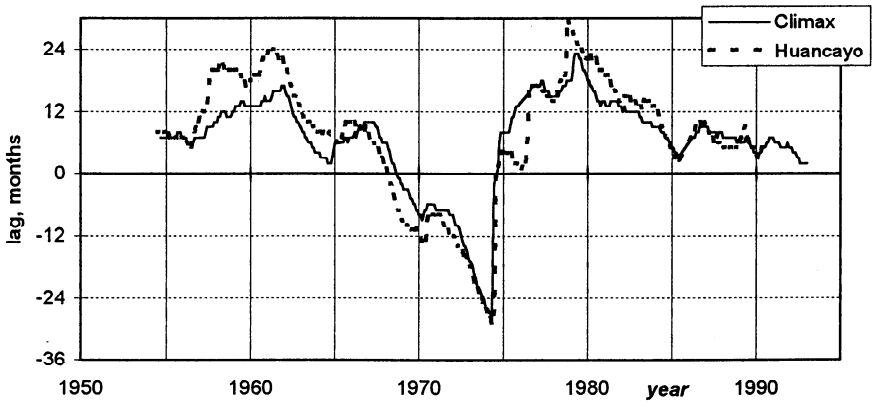

Figure 8. Time lag between the moments of equal phases of SA and CR (Climax NM, solid line and Huancayo NM, dashed line) cycles.

series (Figure 1a) that the CR intensity reached the maximum of cycle 20 as early as in 1972 and remained at that level until the beginning of next cycle, while the minimum of SA was reached only in 1976.

The time profile of the running cross-correlation coefficient between CR and SA series was found to be very similar (except for the particular period of 1972-1977) for neutron monitors with different geomagnetic cutoff rigidities (Figure 2b). This implies that the modulation of CR particles of different energy (rigidity) has a similar overall behavior although the depth of modulation depends on particle energy. This is also supported by the fact that the general behavior of smoothed CR intensity (Figure 9) as recorded by midlatitude Climax and equatorial Huancayo monitors (the data are scaled for better comparison) is similar during the entire period studied except for 1970-1977. This similarity does not contradict the model calculations of CR modulation. For example, time profiles of calculated intensities for 1 GeV and 10 GeV protons [*Le Roux and Potgieter,* 1992, Figure 3] are similar when scaled as given in our Figure 9. Therefore the modulation of CR particles of different energy is driven on the same timescale and the same spatial scale by the same heliospheric processes, which may be merged interaction regions [e.g., *Perko and Burlaga,* 1992; *Burlaga et al.,* 1993], waviness of the heliospheric neutral sheet [e.g., *Kota and Jokipii,* 1983; *Le Roux and Potgieter,* 1992] or multiple solar eruptions [*Cliver and Cane,* 1996]. (We study here long-term global processes. Short-time variations like solar proton events or Forbush decreases are beyond the scope of the present study.)

As noted above, a strong energy (rigidity) dependence of modulation is found in the descending phase of cycle 20 (Figure 2b). The intensity of CR particles with rigidity harder than 13 GV (Huancayo NM) was independent of SA during 1973-1976. Correlation between SA and CR of lower energy was also weak for a longer time than usual, about 4 years compared to 1-1.5 years of an average cycle. The fact that the negative correlation was systematically weaker for Climax (3 GV) than for Oulu (<1 GV) monitor serves as additional indication for energy dependence of modulation.

The CR modulation is controlled by the global solar activity affecting the conditions of CR propagation in the heliosphere. Most likely, the very low SA of cycle 20 is responsible for the unusual properties found. This implies that the perturbation of

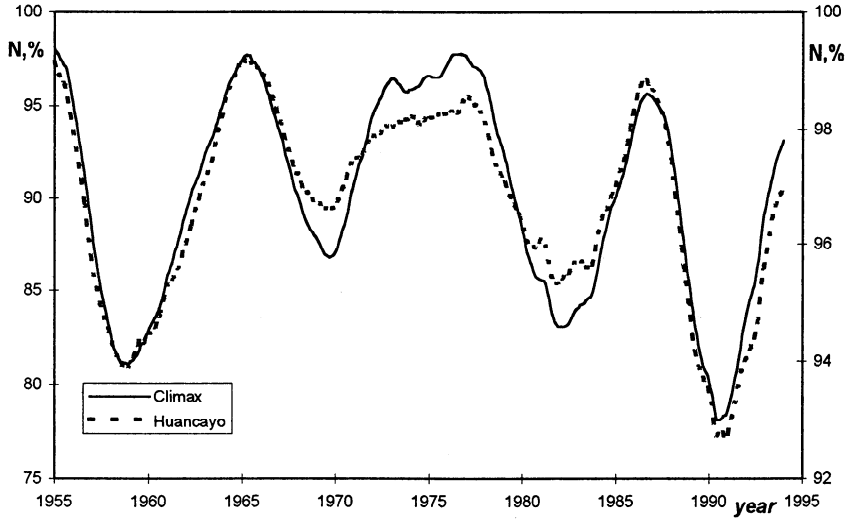

Figure 9. Smoothed count rates of Climax (solid line, left axis) and Huancayo (dashed line, right axis) neutron monitors.

the heliosphere is weaker and less widely spread during cycle 20 than during other cycles. This might lead to a situation where the heliospheric perturbations are relatively "thin" for higher energy particles (Huancayo monitor in our case), allowing those particles to reach Earth as if it was a minimum SA period. However, the perturbations still could be "thick" enough for lower-energy particles (Climax and Oulu NMs) to be driven by the weak SA. Such a situation could result in energy dependence of modulation as well as other peculiarities found. Thus the heliosphere recovered after the 20th maximum more quickly than usual. This implies that the heliospheric perturbations caused by SA in the descending phase of cycle 20 were quite local and could not result in global modulation of CR. Therefore CR had already reached its maximum level in 1972, although the actual SA minimum was found only in 1976. It is also known that the solar dipole tilt decreased very rapidly from the maximum level of about 90° in late 1970 to about 30° in 1971 [*Wang,* 1993] and that the heliospheric neutral sheet was very flat as early as 1973 (and probably even earlier) [e.g., *Kojima and Kakinuma,* 1990]. These results demonstrate that the heliosphere reached the quiet time structure very early in the declining phase of cycle 20, implying an exceptionally fast recovery of the CR level and a long flat CR maximum during 1972-1977.

Concluding, we have shown that the overall behavior of CR modulation by SA is essentially similar for CR particles of different energies within the neutron monitor energy range during most of the four recent solar cycles. We have studied the evolution of CR and SA cycles in a 3-D phase space. The SA cycles are very regular and planar, but the evolution of CR cycles is more complicated. The CR cycles are also planar, except for CR cycle 20 which is significantly 3-D. We have also studied the time behavior of the momentary phase for CR and SA cycles. A comparative analysis of the CR and SA cycles evolution shows that while the CR evolution mostly follows the SA evolution, a period of unusual modulation is found in the 1970s. It is probable that although the SA was of average level (and even a very strong solar event of August 1972 occurred), the expansion of the SA-related perturbations in the heliosphere was not wide enough to effectively modulate CR particles within the neutron monitor energy range, leading to the observed singularities in the CR modulation in the descending phase of cycle 20.

Acknowledgments. NOAA is acknowledged for sunspot number data, and WDC-C2 is acknowledged for neutron monitor data. The authors thank the Academy of Finland and Centre for International Mobility (CIMO) for financial support.

The Editor thanks one referee for his assistance in evaluating this paper.

References

Burlaga, L. F., F. B. McDonald, and N. F. Ness, Cosmic ray modulation and the distant heliospheric magnetic field: Voyager 1 and 2 observations from 1986 to 1989, *J. Geophys. Res. 98(1)*, 1, 1993.

Cliver, E. W., and H. V. Cane, The angular extents of solar interplanetary disturbances and modulation of galactic cosmic rays, *J. Geophys. Res., 101(7)*, 15533, 1996.

Dorman, I. V., and L. I. Dorman, Solar wind properties obtained from the study of the 11-year cosmic ray cycle, 1, *J. Geophys. Res., 72(5)*, 1513, 1967.

Kojima, M., and T. Kakinuma, Solar cycle dependence of global distribution of solar wind speed, *Space Sci. Rev., 53*, 173, 1990.

Kota, J., and J. R. Jokipii, Effects of drift on the transport of cosmic rays, VI, A three-dimensional model including diffusion, *Astrophys. J., 265*, 573, 1983.

Kremliovsky, M. N., Can we understand time scales of solar activity? *Sol. Phys., 151*, 351, 1994.

Kurths, J., and A. A. Ruzmaikin, On forecasting the sunspot numbers, *Sol. Phys., 126*, 407, 1990.

Le Roux, J. A., and M. S. Potgieter, The simulated features of heliospheric cosmic-ray modulation with a time-dependent drift model, II, On the energy dependence of the onset of new modulation in 1987, *Astrophys. J., 390*, 661, 1992.

Lopate, C., and J. A. Simpson, Cosmic ray heliospheric propagation during 22-year solar magnetic field cycle, *Conf. Pap. Int. Cosmic Ray Conf. 22nd, 3*, 493, 1991.

Mundt, M. D., H. W. B. Maguire II, and R. P. Chase, Chaos in the sunspot cycle: Analysis and prediction, *J. Geophys. Res., 96(2)*, 1705, 1991.

Mursula, K., I. G. Usoskin, and B. Zieger, On the claimed 5.5-year periodicity in solar activity, *Sol. Phys., 176*, 201, 1997.

Nagashima, K., and I. Morishita, Twenty-two year modulation of cosmic rays associated with polarity reversal of polar magnetic field of the Sun, *Conf. Pap. Int. Cosmic Ray Conf. 16th, 3*, 325, 1979.

Nymmik, R. A., and A. A. Suslov, Characteristics of galactic cosmic ray flux lag times in the course of solar modulation, *Adv. Space Res., 16(9)*, 217, 1995.

Ostryakov, V. M., and I. G. Usoskin, On the dimension of solar attractor, *Sol. Phys., 127*, 405, 1990.

Packard, N. H., J. P. Crutchfield, J. D. Farmer, and R. S. Show, Geometry from a time series, *Phys. Rev. Lett., 45*, 712, 1980.

Perko, J. S., and L. F. Burlaga, Intensity variations in the interplanetary magnetic field measured by Voyager 2 and the 11-year solar cycle modulation of galactic cosmic rays, *J. Geophys. Res., 97(4)*, 4305, 1992.

Takens, F., *Lecture Notes in Mathematics,* vol. 898, p. 366, Springer-Verlag, New York, 1981.

Usoskin, I. G., G. A. Kovaltsov, H. Kananen, K. Mursula, and P. Tanskanen, Phase evolution of solar activity and cosmic-ray variation cycles, *Sol. Phys., 170*, 447, 1997.

Wang, Y.-M., On the latitude and solar cycle dependence of the interplanetary magnetic field strength, *J. Geophys. Res., 98(3)*, 3529, 1993.

Webber, W. R., and J. A. Lockwood, Characteristics of the 22-year modulation of cosmic rays as seen by neutron monitors, *J. Geophys. Res., 93(8)*, 8735, 1988.

H. Kananen, K. Mursula, and P. Tanskanen, Department of Physical Sciences, University of Oulu, Linnanmaa, FIN-90570 Oulu, Finland. (e-mail: hannu.kananen@oulu.fi; kalevi.mursula@oulu.fi; pekka.tanskanen@oulu.fi)

G.A. Kovaltsov, A. F. Ioffe Physical-Technical Institute, 194021 St. Petersburg, Russia. (e-mail: koval@nspl.ioffe.rssi.ru)

I.G. Usoskin, Sezione de Milano, Istituto Nazionale di Fizica Nucleare, Via Celoria 16, 20133 Milano, Italy. (e-mail:usoskin@hpamsmi1.mi.infn.it)

(Received September 22, 1997; revised December 19, 1997; accepted December 19, 1997.)